Characterization of Rodlike Aggregates Generated from a Cationic Surfactant and a Polymerizable Counterion

Michael J. Gerber,[†] Steven R. Kline,[‡] and Lynn M. Walker*,[†]

Department of Chemical Engineering (Center for Complex Fluids Engineering), Carnegie Mellon University, Pittsburgh, Pennsylvania 15213 and NIST Center for Neutron Research, National Institute of Standards and Technology, Gaithersburg, Maryland 20899

Received April 29, 2004. In Final Form: July 15, 2004

The polymerization of elongated micellar structures offers a novel approach to the production of high-aspect-ratio, water-soluble amphiphilic nanorods. A cationic surfactant with a vinyl-containing counterion, cetyltrimethylammonium 4-vinylbenzoate, has been synthesized and polymerized to produce high-aspect-ratio nanoparticles which are insensitive to changes in solution conditions. Aggregates are polymerized over a range of initiator concentrations allowing for control of the product length. Small-angle neutron scattering and light scattering are used to characterize the dimensions of the polymerized aggregates, showing them to have a fixed radius of 2 nm and contour lengths varying from 96 to 340 nm. Proton NMR verifies the chemical structure and provides insight into the mobility of the aggregate components. Finally, gel permeation chromatography of the polymer extracted from the aggregates indicates that the polymerization reaction controls the aggregate dimensions.

Introduction

The addition of hydrotropic counterions to ionic surfactant systems often leads to the formation of elongated, or wormlike, micelles at only a few times the critical micelle concentration.[1] These wormlike micelles form viscoelastic solutions, retain the solubilizing properties common to surfactant systems, and provide a unique anisotropic template for materials processing.

The structure of these living polymer systems is defined by a precarious balance of hydrophobic and electrostatic forces. This balance causes the micelle dimensions to be a strong function of many system variables. For example, the length of the micelles increases with increasing surfactant concentration and decreases with increasing temperature.[1−4] Thus, small variations in system conditions affect micelle dynamics and dimensions, limiting many applications of these materials, especially those involving multistep processing.

To maintain the amphipilic nature of the living system and make use of the self-assembled structure to generate aggregates with stable, predictable nanoscale structure, the inclusion of polymerizable moieties has been utilized.[5] Polymerization of surfactants has successfully captured the structure of spherical micelles in both ionic and nonionic surfactants.[6,7] Here, we propose to generate larger, anisotropic aggregates through the polymerization of counterions on wormlike micelles.

The resulting polymerized aggregates, with a combination of high-aspect-ratio and amphiphilic behavior, have potential in several exciting applications. For example, we have explored the use of these rods in the formation of structured layers irreversibly adsorbed to hydrophilic surfaces.[8,9]

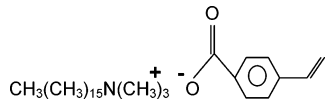

Figure 1. Chemical Structure of surfactant (CTA^+) and counterion (VB^-)

However, before further pursuit of these applications, we must be able to predict and control aggregate lengths and determine the aggregate structure. To accomplish this, we will synthesize a polymerizable, wormlike-micelle-forming surfactant system consisting of a cationic surfactant and a vinyl-containing counterion and polymerize the micelles formed by this surfactant to yield stable aggregates. We hypothesize that we will be able to control the resulting aggregate structure using the polymerization conditions, and we will characterize the molecular composition and dimensions of these aggregates so that potential applications can be realized. To fully characterize the polymerized micelles, we make use of static light scattering (SLS) to measure the aggregate lengths, NMR to quantify the molecular composition, and gel permeation chromatography (GPC) to determine the molecular-weight distribution of the polyvinyl benzoate (pVB^-) polymer.

Background

There is only one report in the literature of the successful polymerization of wormlike micelles.[10] In that work, a surfactant system with a common cationic surfactant and a vinyl-containing counterion was utilized. Cetyltrimethylammonium 4-vinylbenzoate (CTVB), shown in Figure 1, has been successfully synthesized in a molar ratio of 1:1 surfactant to counterion. This surfactant has been polymerized, resulting in stable, high-aspect-ratio aggregate structures which retain the cross-sectional

* Author to whom correspondence should be addressed. Email: lwalker@andrew.cmu.edu.

[†] Carnegie Mellon University.

[‡] National Institute of Standards and Technology.

(1) Israelachvili, J. N. *Intermolecular and Surface Forces*; Academic Press: London, 1985.

(2) Tanford, C. *The Hydrophobic Effect*; Wiley: New York, 1980.

(3) Lequeux, F. *J. Colloid Interface Sci.* **1996**, *1*, 341.

(4) Truong, M. T. Thesis, Carnegie Mellon University, Pittsburgh, PA, 2002.

(5) Paleos, C. M. *Polymerization in Organized Media*; Gordon and Breach: Philadelphia, 1992.

(6) Summers, M.; Eastoe, J.; Davis, S.; Du, Z. *Langmuir* **2001**, *17*, 5388.

(7) Dufour, M.; Guyot, A. *J. Colloid Polym. Sci.* **2003**, 97.

(8) Biggs, S.; Walker, L. M.; Kline, S. R. *Nano Lett.* **2002**, *2*, 1409.

(9) Biggs, S.; Kline, S. R.; Walker, L. M. *Langmuir* **2004**, *20*, 1085.

(10) Kline, S. R. *Langmuir* **1999**, *15*, 2726.

10.1021/la048929a CCC: $27.50
Published on Web 08/27/2004

structure of the initial micelles.[10] Prior to polymerization, CTVB solutions are clear and viscoelastic. On the basis of other CTA^+ systems with bulky counterions, we expect the system to be composed of flexible, charged wormlike micelles.[4] During the course of the polymerization, the solution passes through a white, turbid phase and then becomes clear again. The turbidity indicates that there is a large-scale rearrangement of the surfactant structure during the reaction. A mechanism for the turbidity has been proposed[11] but its specifics are not important here as that process does not influence the final diameter of the aggregates. The final product of the polymerization is a much less viscous, clear solution containing shorter, rigid micelles. Previous work and current observations show that the polymerized micelles are stable over long times. The aggregate dimensions do not change with the addition of NaCl, after freeze-drying, or through dilution, and the aggregates cannot be broken apart by dialyzing against large gradients of pH or salt.

In previous work, the polymerized CTVB aggregates had been characterized exclusively using small-angle neutron scattering (SANS). SANS data is presented as scattered intensity as a function of normalized scattering angle q, defined as $q \equiv 4\pi/\lambda \sin(\theta/2)$, where λ is the wavelength of incident radiation and θ is the scattering angle. SANS operates over the range of $0.003 < q < 0.2$ $Å^{-1}$, which is ideal for probing small-length scales, from 5 to 300 Å. Previous work on the CTVB system shows that the Coulomb interaction peak present in CTVB solutions vanishes upon polymerization, leading to an assumption that the overall charge on the polymerized CTVB (pCTVB) aggregates is neutral.[10] The pCTVB aggregates have cylindrical cross sections with a radius of 2 nm, the same as the unpolymerized micelles. SANS also shows that the polymerized aggregates are rigid over a significant portion of their length.

Materials and Methods

Cetyltrimethylammonium hydroxide and 4-vinylbenzoic acid were purchased from Fluka (Ronkonkoma, NY). D_2O, 99.9 mol% enriched, potassium iodide, and trimethylsilyldiazomethane were purchased from Sigma-Aldrich (St. Louis, MO). The water-soluble free-radical initiator VA-44 (2,2′-azobis[2-(2-imidazolin-2-yl)-propane] dihydrochloride) was donated by Wako Chemicals (Richmond, VA). All materials were used as received. Water from a reverse osmosis source was purified in a Millipore filtration system immediately before use.

Cetyltrimethylammonium 4-vinylbenzoate (CTVB) was prepared by neutralization of 4-vinylbenzoic acid in the presence of a slight stoichiometric excess of cetyltrimethylammonium hydroxide (CTAOH) using a method described elsewhere.[10] During the neutralization, care was taken that both surfactant and acid solutions were chilled and kept near 10 °C, which is above the Krafft temperature of CTAOH ($T_k < 0$ °C) but below the Krafft temperature of CTVB ($T_k = 19$ °C), allowing the CTVB to precipitate. Solid CTVB was dried and washed twice with cold water and then recrystallized from ethanol to remove any organic impurities.

Samples for polymerization were prepared with water (or D_2O) which was boiled for 10 min to remove residual CO_2 and then cooled under nitrogen (grade 5.0) to deplete any oxygen. The surfactant was dissolved at 60 °C with light stirring under an atmosphere of constantly circulating nitrogen which had been bubbled through water. The reaction was initiated by injecting 1 mL of initiator predissolved in water (or D_2O) into the homogeneous surfactant solution. The initiator concentration will be defined as $[I]$ = % (mol Initiator/mol CTVB). The polymerization was carried out using several initiator concentrations, ranging from $0.5\% < [I] < 10\%$, while the surfactant was kept at a constant concentration of 23 mM CTVB. The reactions were run in a pure nitrogen atmosphere and under constant stirring using a magnetic stir bar. Successful reactions were observed to pass through a turbid phase during the course of the reaction. The resulting clear solution exhibits none of the viscoelasticity of the initial solution and does not precipitate when chilled below the Krafft temperature of CTVB.

Static light scattering experiments were performed using a Brookhaven Instruments Corporation BI-200SM goniometer with a $\lambda = 532$ nm laser source. Scattering was performed at angles between 70° and 135° with 5° increments and sample concentrations between 0.25 and 2 mg/mL. Data were analyzed using the method of Zimm[12] to determine the radii of gyration (R_g), weight average molecular weights (M_w), and second virial coefficients (A_2) of the aggregates. The dn/dc of pCTVB was found to be 2.44×10^{-7} m^3/g in D_2O and 1.89×10^{-7} m^3/g in H_2O using a differential refractometer. Concentrations of all samples were measured using a Spectronic Genesys 2 UV−vis spectrophotometer ($\lambda = 296$ nm) and were based on comparison to standard solutions prepared from dry material.

Small-angle neutron scattering experiments were performed on the NG3 30 m SANS instrument at the NIST Center for Neutron Research in Gaithersburg, MD. A 1.2 cm diameter, collaminated beam of neutrons of wavelength $\lambda = 6$ Å ($\Delta\lambda/\lambda = 0.143$) were incident on either 1- or 2 mm-thick samples in quartz cells. Two sample-to-detector distances were used to give an overall q range of $0.0037 < q < 0.23$ $Å^{-1}$. Sample scattering was corrected for background and empty cell scattering. The corrected data sets were circularly averaged and placed on an absolute scale using procedures and software supplied by NIST.[13]

To study the polymer product itself and to probe the internal structure of the polymerized micelles, the poly(4-vinylbenzoic acid) was stripped from the polymerized micelles by adding 2× molar excess KI. During stripping, the pH was maintained at 9.5 with dilute NaOH to maintain solubility of the pVB polyacid. The polymer was then separated from the precipitated surfactant salt and acidified using HCl at pH 1.0. The polyacid was then washed and separated. To esterify the sample for GPC measurements, the polymer was dissolved in methanol and then reacted with 2.5× molar excess of 2M trimethylsilyldiazomethane in diethyl ether solution.[14] The reaction mixture turns from pale yellow to clear, releasing heat and nitrogen upon successful esterification. The resulting poly-methyl ester was dried and dissolved in THF for GPC measurements. GPC was performed using a series of PSS styrogel columns with pore sizes of 10^5, 10^3, and 10^2 Å and a Waters 2410 differential refractometer detector. The column was calibrated to polystyrene standards between 400 and 2×10^6 g/mol and uses an internal toluene elution standard.

NMR experiments were performed on a Bruker WM-300 NMR instrument using a MacSpec Tecmag console. Samples were dissolved in D_2O or, when appropriate, deuterated chloroform. Data were reduced using software provided by Acorn NMR.[15]

Results

Chemical Analysis. NMR is used as a quantitative verification of the chemical composition of the polymerized aggregates at various processing stages, as well as a qualitative measure of component mobility in the aggregates, or micelle dynamics. Figure 2a shows the proton NMR spectrum for a sample of unpolymerized CTVB. The peaks from left to right represent the protons on aromatic groups (~7.9 and 7.3 ppm), the vinyl groups (~6.6, 5.7, and 5.2 ppm), D_2O (~4.8 ppm), the methylammonium groups (~3 ppm), and the alkyl groups (~1−2 ppm). The peaks of this spectrum appear very broad, an effect attributed to hindered mobility of the molecules within the self-assembled structures. The possibility of peak

(11) Kline, S. R. *J. Appl. Cryst.* **2000**, *33*, 618.

(12) Zimm, B. H. *J. Chem. Phys.* **1948**, *16*, 1099.

(13) *SANS Data Reduction and Imaging Software*; NIST: Gaithersburg, MD, 1998.

(14) Hashimoto, N.; Aoyama, T.; Shiori, T. *Chem. Pharm. Bull.* **1981**, *29*, 1475.

(15) NUTS NMR Data Processing Software; AcornNMR: Livermore, CA, 2003.

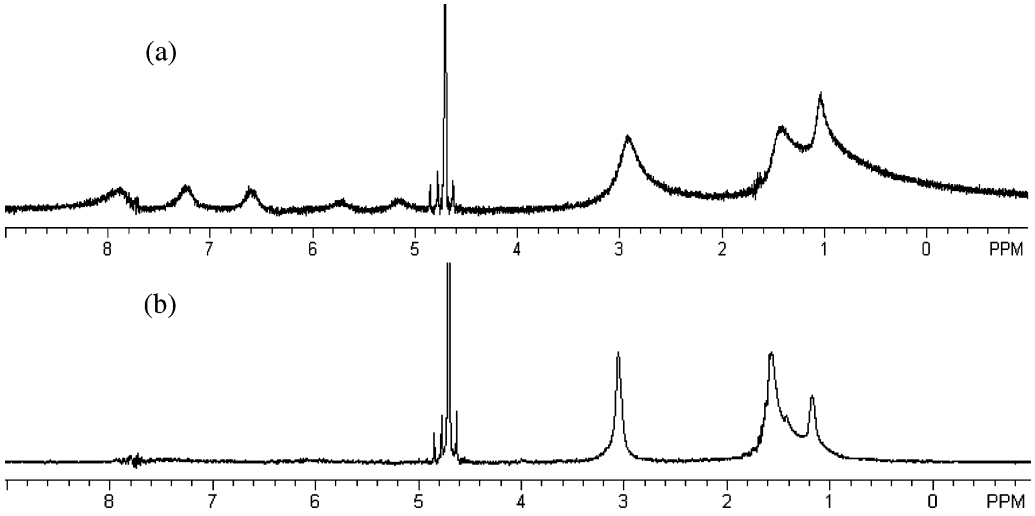

Figure 2. (a) NMR spectrum of 10 mg/mL CTVB in D_2O (unpolymerized). (b) NMR spectrum of 10 mg/mL pCTVB ([*I*] = 5%).

broadening due to solution viscosity is negated as the peaks remain broad on dilution of the surfactant.[16] The five peaks representing the 4-vinylbenzoic acid, except for the aromatic proton adjacent to the carboxylic acid, are upshifted relative to NMR spectra of 4-vinylbenzoic acid provided by the manufacturer, indicating their presence in the organic core of the micelle. This result agrees with existing work which shows the position of aromatic counterions in CTA^+ micelles to be at the interface between the aqueous and hydrophobic regions.[17]

Figure 2b shows the same CTVB sample after polymerization using [*I*] = 5%. Only three peaks are present, the hydrocarbon protons, methylammonium protons, and D_2O protons. The alkyl peak (~1−2 ppm) grows and the relative intensities of the two large peaks invert. The change in the ratio of areas under the alkyl and the methane peaks is not quantitative enough to yield useful information. While the disappearance of the vinyl signal seems to indicate high conversion, it is coupled with the complete loss of the aromatic peaks. This signal loss is the result of a drastic change in molecular mobility of the counterions after polymerization relative to the NMR time scale. The polymerization effectively obstructs the dissociation of counterions out of the aggregates, leaving the polymer constituents significantly immobilized in the aggregate and making them invisible to solution NMR. Meanwhile, the surfactant peaks become sharper, indicating greater mobility, and they experience a slight downfield shift, indicating their presence in a more polar environment.[17,18] Thus, even though the polymer is trapped in the aggregates, the CTA^+ surfactant is still free to dissociate and has greater abundance in the bulk aqueous phase than before the polymerization.

NMR spectra were also collected for samples of the counterion polymer alone, dissolved in deuterated chloroform, after the removal of the surfactant using the stripping process described above. After computing the integrals under the resulting peaks, the ratio of the aromatic to alkyl peaks was found to be 4:3.05, which is the expected value for a vinyl benzoate polymer (4:3). The end group, which consists of a bound initiator molecule, appears as a sharp peak at 4 ppm. One polymer sample was fractionated, removing all high-molecular-weight polymers. End-group analysis of this spectrum yields an average degree of polymerization of 10. Thus, a population of oligimers is present in the aggregates after polymerization. The presence of these oligimers will be further verified using GPC.

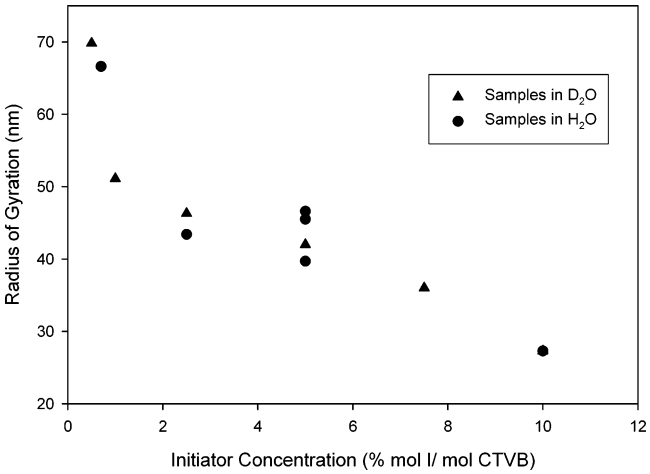

Figure 3. Radius of gyration (SLS) of aggregates prepared with varying initiator concentration in two different solvents.

Structural Analysis of the Aggregates. To characterize the dimensions of the polymerized aggregates formed, a Zimm analysis of static light scattering is employed. The polymerized aggregates scatter well and yield data that is linear as both a function of concentration and scattering angle. An extrapolation of the data produces curves for both zero-angle and zero-concentration scattering. These curves are fit by least-squares regression, with average R^2 values of 0.98 and values no lower than 0.95 for all samples.

Figure 3 shows the radius of gyration (R_g) obtained from a Zimm analysis of SLS data obtained from pCTVB aggregates polymerized with various initiator concentrations. The R_g decreases monotonically with increasing [*I*], with values ranging from 28 to 70 nm, representing small-scale colloidal particles. Each data point in Figure 3 represents analysis of a sample from a separate polymerization, and the plot shows samples prepared in both D_2O (triangles) and H_2O (circles). There is no clear distinction between samples polymerized in these two different solvents. Quantitatively, reproducibility of our polymerization process is expressed by the four samples

(16) Nakagawa, T.; Tokiwa, F. Nuclear Magnetic Resonance of Surfactant Solutions. In *Surace and Colloid Science*; Matijevic, E., Ed.; John Wiley & Sons: New York, 1976; Vol. 9, p 69.
(17) Kreke, P. J.; Magid, L. J.; Gee, J. C. *Langmuir* **1996**, *12*, 699.
(18) Eriksson, J. C.; Gilbert, G. *Acta Chem. Scand.* **1966**, *20*, 2019.

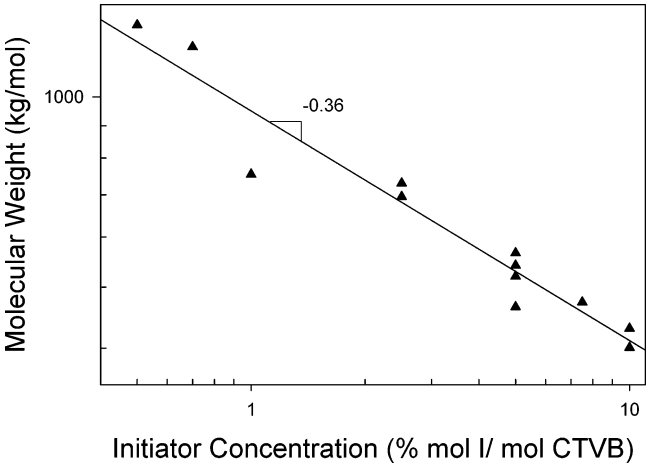

Figure 4. Aggregate molecular weight (SLS) with varying initiator concentration. The line indicates power law dependence.

initiated at $[I] = 5\%$, which have an average R_g of 43.5 nm with a standard deviation of 6%.

SLS also provides an independent measurement of the weight-average aggregate molecular weight, shown in Figure 4 as a function of initiator concentration. This is the molecular weight of the entire aggregate including the pVB polymer (~34 wt % assuming 1:1 VB^- monomer to CTA^+ surfactant) and the CTA^+ surfactant. M_w decreases monotonically with increasing initiator concentration. Thus, varying the initiator concentration allows for control of the aggregate M_w over a wide range, nearly a decade for the initiator concentration range studied.

The relationship between molecular weight and initiator concentration provides insight to the kinetic mechanism, but there is not enough data to specifically identify the kinetics. The regression of the data provides a relationship of $M_w \propto [I]^{-0.36}$, as shown in Figure 4. Thus, the polymerized micelle reaction has a weaker dependence on initiator concentration than bulk free radical polymerization,[19] which has a power law dependence of -1. This result is reasonable since the mechanism of this reaction is quite different. Rather than being dominated by the frequency of molecular collisions, the aggregate polymerization depends mostly on the entrance of free radicals (the initiator is water soluble) into the hydrophobic phase of the micelles and on the arrangement and mobility of monomer within the micelle. A similar dependence of M_w on $[I]$ is observed for other reactions in which the monomer feed is controlled, such as in the microemulsion polymerization of styrene, where the exponent has values between -0.5 and -0.4.[20,21]

A comparison between the two measured properties (molecular weight and radius of gyration) provides qualitative information about the aggregate shape. The molecular weight varies linearly with R_g, as shown in Figure 5. This linear proportionality between mass and the characteristic dimension is indicative of rodlike aggregates. If the aggregates are assumed to be rigid rods, the R_g measured corresponds to rigid rod lengths between 96 and 241 nm, as summarized in Table 1. Thus, these 2 nm-radius particles can be produced with aspect ratios (L/d) as high as 60. The linear relation shown in Figure 5 is developed excluding the high $[I]$ (10%) data. The reason for this omission will be discussed below.

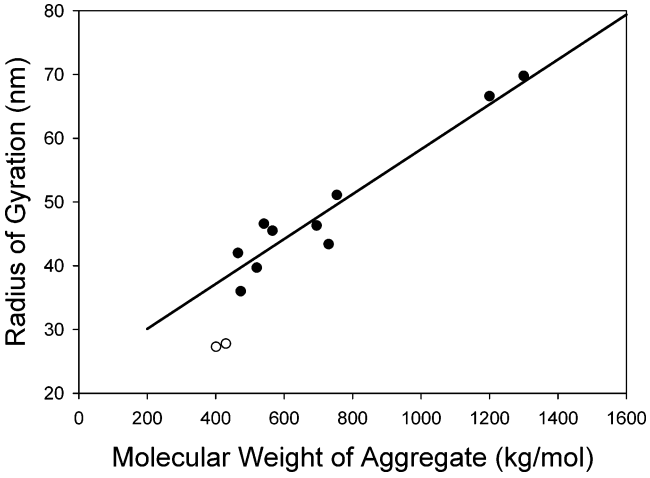

Figure 5. Radius of gyration of aggregates as a function of molecular weight, both measured with SLS. Linear fit of data excluding data polymerized at $[I] = 10\%$.

Table 1. Properties of Polymerized Aggregates Measured via SLS.[a]

$[I]$ %	R_g (nm)	aggregate M_w (g/mol)	Rod Length (nm)
0.5	69.6	1.3E+06	241 ± 14
0.7	66.6	1.2E+06	231 ± 14
1.0	51.1	7.5E+05	177 ± 11
2.5	46.2	7.0E+05	160 ± 10
5.0	43.5	5.2E+05	145 ± 9
7.5	36.0	4.7E+05	124 ± 7
10.0	27.7	4.2E+05	96 ± 5

[a] Rod lengths are calculated from the radius of gyration assuming a rigid rod.

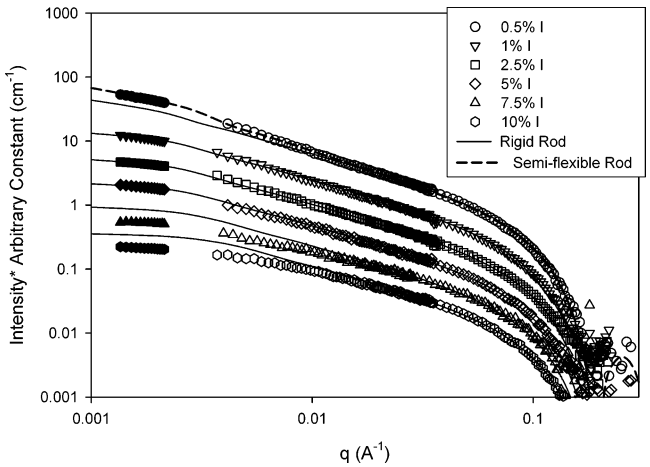

Figure 6. Small-angle neutron scattering (open symbols) and static light scattering (filled symbols) results for 1 mg/mL pCTVB micelles polymerized using varying initiator concentrations. The solid curves are the predicted scattering function for monodisperse rigid rods using 2 nm radius and length determined from SLS. The dashed curve is the predicted scattering function for a semi-flexible rod with a 2 nm radius and a radius of gyration determined by SLS. An arbitrary vertical shift is applied to each data set. The error on each point is within the marker for $q < 0.15$.

To further quantify the overall structure of the polymerized aggregates, small-angle neutron scattering (SANS) is employed. Figure 6 shows the scattering intensity, $I(q)$, dependence of both neutron (open symbols) and light (filled symbols) scattering for a set of 1 mg/mL pCTVB samples polymerized using varying initiator concentrations. Note that these samples were all polymerized from 10 mg/mL

(19) Flory, P. J. *Principles of Polymer Chemistry*; Cornell University Press: Ithica, 1953.
(20) Puig, J. E.; Perez-Luna, V. H.; Perez-Gonzalez, M.; Macias, E. R.; Rodriguez, B. E.; Kaler, E. W. *Colloid Polymer Sci.* **1993**, *271*, 114.
(21) Guo, J. S.; Sudol, E. D.; Vanderhoff, J. W.; El-Aasser, M. S. *J. Polym. Sci., Part A: Polym. Chem* **1992**, *30*, 703.

CTVB solutions in D_2O and then diluted for SANS. The light scattering has been vertically shifted to appear on the same absolute scale as the neutron scattering, and all of the plots have been vertically shifted by an arbitrary constant to aid in viewing and comparison. All curves show a distinct q^{-1} region indicative of rigid rods and a steeper q-dependence at high-q due to the finite cross-section of the micelles.[22]

Scattering data is modeled using the form factor, $P(q)$, for a monodisperse rigid cylinder[22] (solid lines). This model has only two parameters: the radius, which has a constant value of 2 nm set by the surfactant tails, and the aggregate length. We utilize the lengths obtained from SLS and given in Table 1. The monodisperse model corresponds well to the SANS data, especially for intermediate initiator concentrations ($\sqrt{\chi^2/N} = 1.27$ for the 1% [I] sample). Note that this is not a fitted model, but rather a calculation based on the length derived from SLS and a fixed radius of 2 nm. A model that incorporates polydispersity of length based on a Schultz distribution[23] does not improve the fit of the data, especially for the low [I] samples. The SANS data is only sensitive to polydispersity of length at low-q, and the predicted shift in the form factor due to polydispersity would increase the low-q scattering, which does not match the data.

The upturn in the data at low-q for the longest sample (0.5% I) can be explained by incorporating flexibility into the scattering model. A model prediction for this sample was generated by using a semi-flexible rod form-factor model[24] (dashed line). Once again, the prediction was based on the SLS data. The R_g was fixed to the value obtained from light scattering, and a chi-squared optimization was used to determine a contour length of 340 ± 10 nm and a Kuhn (statistical segment) length of 155 ± 10 nm for the 0.5% I sample. Note that these fit parameters were extracted from an optimization of both the R_g measured directly from SLS and the full $I(q)$ from SANS. The same process was repeated for the three longer samples, yielding a constant Kuhn length of 155 nm. While the longer polymerized aggregates have been shown to have some flexibility, they still have large regions of rigidity, as the longest aggregate has a contour length of only twice the Kuhn length.

Figure 7 shows the same data represented in a Holtzer (bending rod) plot. This representation makes the rodlike nature of the aggregates very clear. The q^{-1} region appears as a constant value of $qI(q)$ on a Holtzer plot, evidenced by the long, flat plateau in the range $0.004 < q < 0.04$ Å^{-1}, which is indicative of rigid regions in the micelle. This plot also clarifies the negative deviations of the scattering from the rod model at low-q. The observed downturn of the high [I] samples cannot be fit with the form-factor model by adjusting the length, the only free parameter. The downturn is also inconsistent with the deviations predicted by including polydispersity or flexibility in the model. Rather, the downturn is similar in nature to that observed for SANS of more concentrated samples. Thus, the negative deviation from the form-factor model is most probably due to structure factor effects, such as interparticle interactions. Assuming a monodisperse distribution, at 1 mg/mL, the interparticle spacing for all samples is on the order of the rod length and is therefore close to the transition from dilute to semidilute behavior.[25] Given the polydispersity of the aggregates, however, such an estimate of behavior is unreliable. The interparticle effects are more pronounced for the high [I] samples because, given a constant molar concentration of surfactant, these shorter aggregates have a higher number density. Thus, we anticipate that SANS at 1 mg/mL is not dilute for the [I] = 7.5% or [I] = 10% samples.

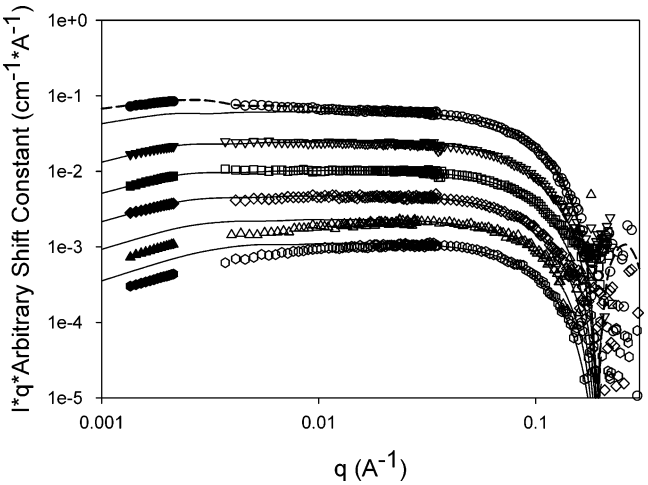

Figure 7. Holtzer (bending rod) plot of dilute SANS scattering with the monodisperse rigid rod and semi-flexible rod form factors. Graphs are vertically shifted to aid viewing. The symbols are the same as those in Figure 6.

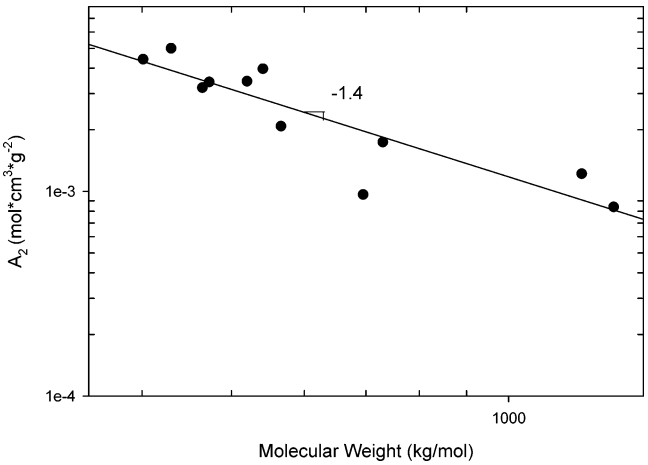

Figure 8. Second virial coefficient (SLS) as a function of aggregate molecular weight.

Solution Behavior. The magnitude of interparticle interactions between the polymerized aggregates in solution is elucidated by measuring the second virial coefficient (A_2). Figure 8 shows A_2 as a function of the molecular weight of the aggregate, with both values being measured using SLS. The A_2 values are positive, indicating that the interactions present are repulsive.[26] The values decrease exponentially with increasing aggregate molecular weight. The resulting exponential relationship indicates that charge repulsions are present in the system because other interactions are not consistent with the observed data. For example, if steric interactions or excluded volume, were the only cause for the repulsion, the A_2 values would

(22) Higgins, J. S.; Benoit, H. C. *Polymers and Neutron Scattering*; Clarendon Press: Oxford, 1994.
(23) Kratochvil, P. Particle Scattering Functions. In *Light Scattering from Polymer Solutions*; Huglin, M. B., Ed.; Academic Press: London, 1972; p 334.
(24) Pedersen, J. S.; Schurtenberger, P. *Macromolecules* **1996**, *29*, 7602.
(25) Doi, M.; Edwards, S. F. *The Theory of Polymer Dynamics*; Clarendon Press: Oxford, 1986.
(26) Evans, D. F.; Wennerstrom, H. *The Colloidal Domain*; Wiley-VCH: New York, 1999.

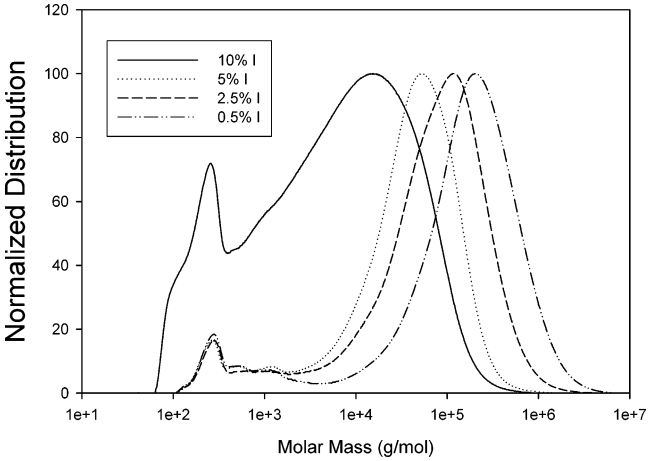

Figure 9. Normalized molecular weight distributrion (based on polystyrene standards) of stripped esterified polyvinylbenzoic acid polymer.

be constant for all aggregate sizes.[27] Similarly, flexibility alone could not produce this result, as a fully flexible chain (an ideal random coil) would result in a slope of only −0.4, as opposed to the observed −1.4. Thus, the large repulsions observed must be a result of electrostatic interactions.

Polymer Molecular Weight. To study the polymer product itself and to explore the internal structure of the aggregates, the CTA^+ is stripped off the aggregates and the polyvinyl benzoate polymer (pVB) is collected. This process is difficult due to the highly stable nature of the polymerized micelles. Neither dialysis methods under high or low pH nor high concentration of NaCl are effective at breaking the aggregates. Instead, the CTA^+ is removed with the addition of potassium iodide, KI. The iodide binds to CTA^+, generating an insoluble ion pair at room temperature and allowing for separation of the polymer. The methyl ester of the polymer is then synthesized by acidifying the pVB^- and reacting with methanol and trimethylsilyldiazomethane.[14] The esterified polymer is dissolved in THF and analyzed using GPC.

Figure 9 shows the normalized molecular-weight distribution of these samples measured using GPC based on polystyrene standards. The polymer has a broad distribution and shows the formation of some fraction of high-molecular-weight polymer of greater than 10^6 g/mol. There is a large peak at low M_w near 200 g/mol (the molecular weight of the esterified VB monomer is 162 g/mol). However, the GPC is not calibrated to measure the molecular weight of particles with such long elution times. Therefore, it is difficult to discern the details of the distribution of small particles, which may consist of monomers, initiator bound monomers, dimers, and small oligimers, whose presence was predicted in our NMR studies. Nevertheless, an effective fractional conversion, shown in Table 2, is extracted by taking the ratio between the integral under the large peak and the area under both peaks. For most samples, this conversion is approximately 96%, which is reasonable for a free-radical polymerization. High conversion is achievable because, despite the electrostatic and solvent hindrances experienced by the counterions, the majority is confined to the micelle core and in contact with a growing polymer chain. We assume that the reaction maintains a high efficiency because the monomer is held at high local concentrations in a structured environment where the monomer units are locally aligned along the surface of the aggregate. This structure promotes polymer growth, resulting in the high conversion observed. For this reason, the wormlike micelle offers an appealing template for polyelectrolyte growth.

Table 2. Polydispersity Index, or PDI, and Conversion {(Initial Moles CTVB − Unreacted Moles Monomer)/(Initial Moles CTVB)} of Polymer Extracted from Aggregates as a Function of Initiator Concentration

[*I*] %	M_w (g/mol)	PDI	% conversion
0.5	3.2E+05	3.0	95.7
1.0	2.6E+05	3.9	91.4
2.5	1.5E+05	2.9	96.3
5.0	7.0E+04	2.3	95.8
7.5	7.6E+04	3.1	96.0
10.0	6.3E+04	2.7	84.1

The [*I*] = 10% sample only reached 86% conversion, as evidenced by the large area under the small-particle peak. This result is expected because a large overabundance of initiator leads to more chains started and terminated quickly, resulting in a high concentration of oligimers. The lack of "complete" conversion would reduce the concentration of rod-stabilizing polymer chains and allow for the formation of some short or even spherical micelles. Thus, we doubt that the [*I*] = 10% sample is composed entirely of rods. Such a distribution of aggregate shapes would depress the observed R_g value, which is why this sample was not included in the regression of Figure 6. Thus, we consider [*I*] = 10% to represent a lower limit on the length of rodlike aggregates that can be produced and an upper limit on the initiator concentration for this polymerization mechanism.

By removing the monomer peak from the data, the molecular-weight distribution of the polymer chains is determined. From this distribution, we extract a polydispersity index (PDI) for the pVB polymer, defined as M_w/M_n. The PDI in this system ranges from 2 to 3.9, which is reasonable for a free-radical polymerization.[28] The PDI and conversion data is summarized in Table 2. Note that this is the polydispersity of the entrained polymer after being removed from the CTVB aggegates, not of the aggregates themselves.

Discussion

If we assume that the polymers exist within the aggregates in an extended conformation, then an estimate of the polymer contour length can be calculated from the GPC data on the basis of carbon bond distances. Figure 10 shows this estimated polymer contour length and the aggregate contour length obtained from the combination of SLS and SANS data as a function of initiator concentration. This approach makes the polymer appear longer than the aggregate. Thus, the extended conformation assumption must be incorrect. Rather, the polymer assumes a more densely packed conformation within the aggregates. More importantly, the estimated length of the polymer and the length of the aggregate are in close agreement and follow the same trend. This result provides evidence that there is a direct correlation between the size of the polymer synthesized and the final length of the polymerized aggregate. Thus, the dimensions of the polymerized micelles are set by controlling the degree of polymerization of the entrained polymer. The pCTVB aggregates are much shorter than the initial CTVB micelles because it is the polymerization reaction, not the micelle condition itself, which dictates the dimensions of the final aggregate.

(27) Wagner, N. J.; Walker, L. M.; Hammouda, B. *Macromolecules* **1995**, *28*, 5075.

(28) Odian, G. *Principles of Polymerization*; McGraw-Hill: New York, 1970.

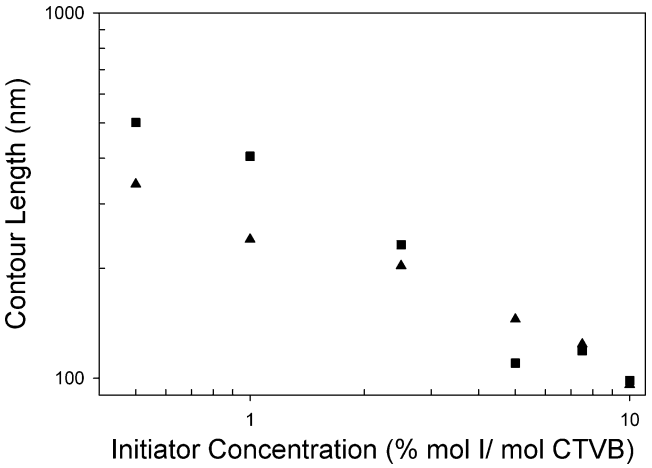

Figure 10. Estimated contour length of the entrained polymer based on GPC measurements and assuming an extended conformation (squares) and contour length of the aggregates measured using SLS and a semi-flexible rod form-factor fit of SANS data (triangles).

This conclusion is also supported by a comparison of the two independent measures of the molecular weights of these aggregates, one from light scattering on the aggregate and the other from GPC on the extracted polymer. While both values once again display a similar dependence on initiator concentration, the polymer component of the molecular weight determined by SLS (34% of the measured value) is greater than the weight-average molecular weight determined from GPC, which we attribute to more than one polymer chain being present in each aggregate. By taking the ratio of the two data sets, we estimate that between one and two chains reside in each micelle.

Through a combination of scattering, GPC, and NMR, we are able to describe the overall structure of the polymerized aggregates in solution. Polymerized CTVB consists of rodlike aggregates made up of an entrained pVB^- polymer, which is rigid and immobile within the core of the aggregate, stabilized by the still-mobile CTA^+ surfactant. The remaining unpolymerized vinyl benzoate monomer and short oligimers also remain mostly within the aggregate, as evidenced by the total disappearance of the VB peaks in NMR. Meanwhile, the surfactant increases its mobility and the ability to disassociate from the aggregates or rearrange along the aggregate surface. More surfactant molecules are present in a polar state, giving evidence of a higher concentration of free surfactant in solution, thereby leaving less than one surfactant molecule per counterion in the aggregates. This condition is logical given the relative solubilities of CTA^+ and vinyl benzoate. At these concentrations, CTA^+ has a high solubility in water, while the polymer and monomers are essentially insoluble and require the aggregate structure to remain in solution. The slight excess of counterions in the polymerized aggregates results in a net negative surface charge, explaining the repulsive interactions observed in the SLS and SANS data. The magnitude of the charge has not yet been measured since standard techniques for measuring ζ-potential are complicated by the small size and rodlike shape of the particles.

The polymerization technique is the only known efficient method of generating the stable, rodlike aggregates discussed in this paper. Neither the acid nor the benzoate form of the polymer can be solubilized easily by other means. Attempts at solubilizing polyvinylbenzoic acid (polymerized outside the micelle phase) with CTAOH take several months because the required ion exchange is hindered by the insoluble polymer. Generating the polymer inside the micelle requires only a few hours.

Conclusions

When polymerized in a wormlike micelle phase, CTVB forms stable polymerized aggregates which are insensitive to changes in surfactant concentration, salt concentration, pH, and temperature. This insensitivity stems from the counterion polymer being immobilized at the surface, or just inside the surface, of the micelle structure and the inability of the counterion to disassociate from the polymerized aggregate. The aggregates are rigid or semi-flexible rods with a fixed radius of 2 nm and varying lengths. The length of the aggregates is defined by the degree of polymerization of the entrained polymer, which is controlled through the initiator concentration during the reaction, allowing for the synthesis of aggregates with aspect ratios between 20 and 60. Each polymerized aggregate has a net negative charge and contains a backbone of one or two sterically hindered polymer chains, which enhance the rigidity of the particles.

Acknowledgment. This work was supported by the National Science Foundation grant CTS-0092967. Light scattering equipment was provided by a grant from the PPG foundation. This work utilized facilities supported in part by the National Science Foundation under Agreement No. DMR-9986442. Certain trade names and company products are identified in order to specify experimental procedures adequately. In no case does such identification imply recommendation or endorsement by the National Institute of Standards and Technology, nor does it imply that the products are necessarily the best available for the purpose.

LA048929A